J|A|C|S
ARTICLES
Published on Web 10/21/2003

Ground-State Conformational Equilibrium and Photochemical Behavior of Syn and Anti *N,N′*-Dimethyl-*N,N′*-di-1-naphthylurea Protophanes

Todd L. Kurth and Frederick D. Lewis*

Contribution from the Department of Chemistry, Northwestern University, Evanston, Illinois 60208-3113

Received January 23, 2003; E-mail: lewis@chem.northwestern.edu

Abstract: The structure, spectroscopy, and photochemistry of *N,N′*-dimethyl-*N,N′*-di-1-naphthylurea have been investigated and compared to the properties of the corresponding secondary diarylurea *N,N′*-di-1-naphthylurea and the tertiary mono arylurea *N,N,N′*-trimethyl-*N′*-1-naphthylurea. The crystal structures and solution NMR spectra of the tertiary and secondary dinaphthylureas establish that they adopt folded (*E,E*) and extended (*Z,Z*) structures, respectively, both in the solid state and in solution. In solution, the tertiary *E,E*-dinaphthylurea exists as a mixture of syn and anti conformations separated by a barrier of ca. 14 kcal/mol, as determined by variable-temperature ^{1}H NMR spectroscopy. Computational exploration of the ground-state potential energy surface suggests that the lowest energy pathway for interconversion of the syn and anti conformers requires concurrent rotation about both the nitrogen−naphthalene and the nitrogen−carbonyl single bonds. The tertiary dinaphthylurea exhibits blue-shifted absorption and red-shifted emission attributed to excitonic interactions between the naphthalene rings. The secondary dinaphthylureas and mono naphthylurea have typical naphthalene-like monomer absorption and fluorescence spectra. Dual exponential fluorescence decay is assigned to the two conformers of the tertiary dinaphthylurea. Nonlinear fitting of the fluorescence decay times provides activation parameters for singlet decay of the two conformers. The decay process is attributed to nonsynchronous naphthalene−naphthalene bonding which, in the case of the syn conformer, results in the formation of a [2+2] intramolecular adduct. The preferred *E,E* conformation and moderate barrier to conformational isomerization make the tertiary dinaphthylurea an attractive building block for larger self-organizing π-stacked aromatic arrays.

Introduction

The through-space electronic interactions between π-stacked aromatic molecules differ from the through-bond interactions of saturated linkers or nonstacked aromatics. For example, the π-stacked base pairs of DNA provide a better medium for superexchange electron transfer than do the σ-bonded pathways of proteins.[1] Interest in the electronic properties of DNA has spurred the interest of this and other laboratories in the electronic interactions of synthetic π-stacked molecules.[2,3] Because $\pi-\pi$ interactions are generally repulsive in the ground state, rigid architectures such as those found in cyclophanes and 1,8-diarylnaphthalenes have traditionally been employed to construct π-stacked molecules.[4] The construction of multilayered systems with these architectures presents formidable synthetic challenges. Less rigid linkers capable of imposing π-stacking offer a potential solution to this problem.[5] Our search for self-folding systems which offer the synthetic flexibility necessary for the construction of extended π-stacked donor−bridge−acceptor systems has led to the study of tertiary *N,N′*-dimethyl-*N,N′*-diarylureas and their poly(arylurea) homologues. The initial objective in this study is the characterization of the structure and electronic interactions in the parent symmetric tertiary diarylureas.[6−8]

Pairwise electronic interactions between π-stacked aromatic molecules are repulsive in the ground state but are often attractive in the singlet excited state. As a consequence of ground-state repulsion, folded conformations of α,ω-diarylalkanes are not populated to a significant extent in the ground

(1) Lewis, F. D.; Liu, J.; Weigel, W.; Rettig, W.; Kurnikov, I. V.; Beratan, D. N. *Proc. Natl. Acad. Sci. U.S.A.* **2002**, *99*, 12536−12541.
(2) (a) Otsubo, T.; Kohda, T.; Misumi, S. *Bull. Chem. Soc. Jpn.* **1980**, *53*, 512−517. (b) Paddon-Row, M. N. *Electron Transfer in Chemistry*; Wiley−VCH: New York, 2001; Vol. 3, pp 179−271. (c) Bartholomew, G. P.; Ledoux, I.; Mukamel, S.; Bazan, G. C.; Zyss, J. *J. Am. Chem. Soc.* **2002**, *124*, 13480−13485. (d) Bartholomew, G. P.; Bazan, G. C. *Acc. Chem. Res.* **2001**, *34*, 30−39. (e) Napper, A. M.; Head, N. J.; Oliver, A. M.; Shephard, M. J.; Paddon-Row, M. N.; Read, I.; Waldeck, D. H. *J. Am. Chem. Soc.* **2002**, *124*, 10171−10181.
(3) (a) Kang, Y. K.; Rubtsov, I. V.; Iovine, P. M.; Chen, J.; Therien, M. J. *J. Am. Chem. Soc.* **2002**, *124*, 8275−8279. (b) Cozzi, F.; Annunziata, R.; Benaglia, M.; Cinquini, M.; Raimondi, L.; Baldridge, K. K.; Siegel, J. S. *Org. Biomol. Chem.* **2003**, *1*, 157−162.
(4) Vögtle, F. *Cyclophane chemistry: synthesis, structures, and reactions*; J. Wiley: Chichester; New York, 1993.
(5) (a) Krebs, F. C.; Jorgensen, M. *J. Org. Chem.* **2002**, *67*, 7511−7518. (b) Yamaguchi, K.; Matsumura, G.; Kagechika, H.; Azumaya, I.; Ito, Y.; Itai, A.; Shudo, K. *J. Am. Chem. Soc.* **1991**, *113*, 5474−5475. (c) Ganis, P.; Avitabil, G.; Benedett, E.; Pedone, C.; Goodman, M. *Proc. Natl. Acad. Sci. U.S.A.* **1970**, *67*, 426.
(6) Lewis, F. D.; Kurth, T. L. *Can. J. Chem.* **2003**, *81*, 770−776.
(7) Lewis, F. D.; Kurth, T. L.; Liu, W. *Photochem. Photobiol.* **2002**, *1*, 30−37.
(8) Kurth, T. L.; Lewis, F. D.; Hattan, C. M.; Reiter, R. C.; Stevenson, C. D. *J. Am. Chem. Soc.* **2003**, *125*, 1460−1461.

10.1021/ja034311w CCC: $25.00

Chart 1

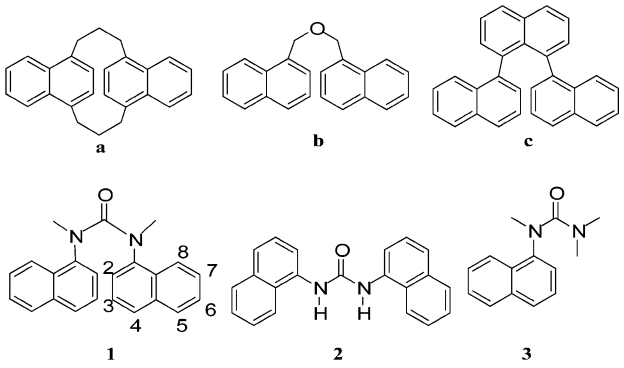

state.[9−11] In a classic study of $\pi-\pi$ interactions, Chandross and co-workers showed that anthracene and naphthalene sandwich dimers could be generated in a low-temperature glass by photochemical cleavage of their [4+4] photodimers. The sandwich dimers diffuse apart upon warming of the glass.[10,12] Cyclophanes with two or more short alkyl linkers can also have π-stacked aromatic rings.[4] A single naphthalene linker suffices to enforce the rigid π-stacked geometry of 1,8-diarylnaphthalenes.[3,13−15] Some *N*,*N*′-dimethyl-*N*,*N*′-diarylureas also adopt folded *E*,*E* confomations in preference to extended *Z*,*Z* or *E*,*Z* conformations.[5] Vögtle refers to singly linked molecules which adopt π-stacked conformations as "protophanes".[4]

Nonsymmetric cyclophanes such as [3.3](1,4)naphthalenophane (Chart 1, a) can exist as a mixture of syn and anti conformers, which differ in the extent of π-overlap and yield different photodimers.[16] Electronic excitation of di-(1-naphthylmethyl)ether (Chart 1, b) results in the formation two photodimers, attributed to the syn and anti intramolecular excimers, which have different photochemical behavior.[17] The syn and anti conformers of 1,8-bis(1-naphthyl)naphthalene (Chart 1, c) have been separated and have a large barrier (27 kcal/mol) for interconversion.[13] Their photochemical behavior has not been investigated.

We report here the results of an investigation of the ground-state structure, electronic spectroscopy, and photochemical behavior of *N*,*N*′-dimethyl-*N*,*N*′-di-1-naphthylurea, **1**. Its structure and spectra are compared to those of *N*,*N*′-di-1-naphthylurea, **2**, and *N*,*N*,*N*′-trimethyl-*N*′-1-naphthylurea, **3** (Chart 1). We have been able to characterize, for the first time, two conformers of a tertiary diarylurea, the *E*,*E*-syn (*E*,*Es*) and *E*,*E*-anti (*E*,*Ea*) conformers of **1**, and to relate their photochemical behavior to their structures.

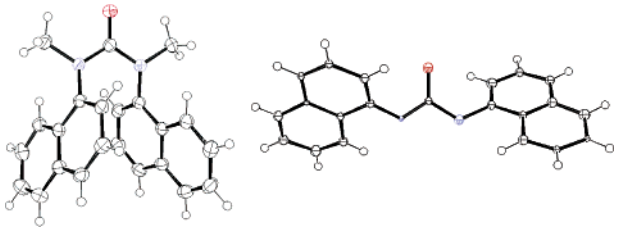

Figure 1. ORTEP drawings of dinaphthylureas **1** (*E*,*Ea*) (left) and **2** (right).

Table 1. Selected Crystallographic Data[a]

	1 (*E*,*Ea*)	**2**
empirical formula	$C_{23}H_{20}N_2O$	$C_{21}H_{16}N_2O$
formula weight	340.42	312.37
crystal color, habit	colorless, block	colorless, plate
crystal system	triclinic	monoclinic
a (Å)	7.9716(13)	4.58(2)
b (Å)	8.516(1)	11.27(3)
c (Å)	13.154(2)	14.71(5)
α (deg)	84.095(3)	
β (deg)	81.398(3)	91.3(8)
γ (deg)	84.421(3)	
space group	*P*-1 (No. 2)	$P2_1$ (No. 4)
Z	2	2
goodness of fit indicator	4.24	9.50
temperature	−120 °C	−120 °C

[a] The remaining parameters are available in the Supporting Information.

Results and Discussion

Ground-State Structures. The synthesis and characterization of **1**−**3** follows published methods which are summarized in the Experimental Section. The tertiary urea **1** crystallizes from hexanes/ethyl acetate as colorless blocks. The crystal structure of the triclinic crystals belongs to the space group *P*-1 (No. 2) with each of the molecules in the unit cell having *E*,*E*-anti (*E*,*Ea*) conformations with identical geometries. The secondary urea **2** is highly insoluble in most solvents. Slow evaporation of a DMSO solution yielded thin colorless needles. The crystal structure of the monoclinic crystals belongs to space group $P2_1$ (No. 4). While the quality of the crystal structure is poor, it suffices to establish that **2** adopts a *Z*,*Z* conformation. ORTEP drawings of a single molecule of *E*,*Ea* and **2** are shown in Figure 1, and the typical crystallographic data are summarized in Table 1.

The crystallization of the dinaphthylureas **1** and **2** in *E*,*E* and *Z*,*Z* conformations, respectively, is analogous to the behavior of several other tertiary and secondary diphenylureas.[18] The urea and naphthalene groups of both **1** and **2** are essentially planar, and the methyl groups in **1** lie in the urea plane. The linear naphthalene short axes (N−C_4) in **1** form a dihedral angle of ca. 60° and a splay angle of 18° about the urea linkage, thus deviating significantly from a true sandwich structure. The large dihedral angle between the urea and naphthalene planes in **2** facilitates intramolecular hydrogen bonding between the carbonyl oxygen and naphthalene H_2, with an O−H_2 distance of <2.7 Å.[19]

Variable-Temperature ^{1}H NMR Spectra of 1. At room temperature, the spectrum of **1** consists of extremely broadened aromatic peaks and a single high field peak corresponding to equivalent urea methyl groups. At elevated temperatures (e.g., 323 K), seven broad signals corresponding to seven sets of

(9) (a) Todesco, R.; Vanbockstaele, D.; Gelan, J.; Martens, H.; Put, J.; Deschryver, F. C. *J. Org. Chem.* **1983**, *48*, 4963−4968. (b) Zachariasse, K.; Kuehnle, W. *Z. Phys. Chem. (Munich)* **1976**, *101*, 267−276.
(10) Chandros, E. A.; Dempster, C. J. *J. Am. Chem. Soc.* **1970**, *92*, 3586.
(11) Hayashi, T.; Mataga, N.; Sakata, Y.; Misumi, S.; Morita, M.; Tanaka, J. *J. Am. Chem. Soc.* **1976**, *98*, 5910−5913.
(12) (a) Chandros, E. A. *J. Chem. Phys.* **1965**, *43*, 4175. (b) Chandros, E. A.; Dempster, C. J. *J. Am. Chem. Soc.* **1970**, *92*, 704.
(13) Ibuki, E.; Ozasa, S.; Fujioka, Y.; Mizutani, H. *Bull. Chem. Soc. Jpn.* **1982**, *55*, 845−851.
(14) Cross, W.; Hawkes, G. E.; Kroemer, R. T.; Liedl, K. R.; Loerting, T.; Nasser, R.; Pritchard, R. G.; Steele, M.; Watkinson, M.; Whiting, A. *J. Chem. Soc., Perkin Trans. 2* **2001**, 459−467.
(15) Zoltewicz, J. A.; Maier, N. M.; Lavieri, S.; Ghiviriga, I.; Abboud, K. A.; Fabian, W. M. F. *Tetrahedron* **1997**, *53*, 5379−5388.
(16) Kawabata, T.; Shinmyozu, T.; Inazu, T.; Yoshino, T. *Chem. Lett.* **1979**, 315−318.
(17) Todesco, R.; Gelan, J.; Martens, H.; Put, J.; Boens, N.; De Schryver, F. C. *Tetrahedron Lett.* **1978**, 2815−2818.
(18) Kagechika, H.; Azumaya, I.; Yamaguchi, K.; Shudo, K. *Chem. Pharm. Bull.* **1996**, *44*, 460−462.
(19) See the Supporting Information.

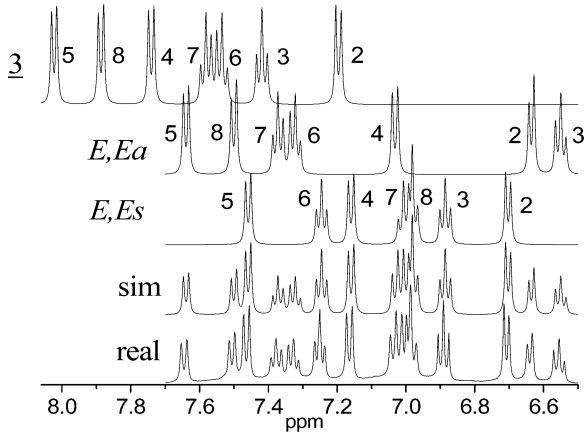

Figure 2. Low-field region of the ^{1}H NMR (500 MHz) spectra of ureas **1** (238 K) and **3** (298 K). The real spectrum of **1** is labeled "real", and the simulated is labeled "sim". The latter consists of *E,Es* and *E,Ea* in a ratio *E,Es*/*E,Ea* of 1/0.6. 3 is simulation of **3**. Labels correspond to those in Chart 1.

naphthalene protons are discernible.[19] Below 260 K, the ^{1}H NMR spectrum of **1** in $CDCl_3$ consists of two sets of aromatic and aliphatic peaks, with unequal integrations, as shown in Figure 2 (real, 238 K). Each set has a multiplet structure similar to that of **3**, which displays four doublets and three triplets at lower field than those of **1**. The NMR spectra of **2** and **3** display no broadening at room temperature, the dimethylamino group of **3** appearing as a singlet.

The two sets of signals for **1** are assigned to the conformers *E,Ea* and *E,Es*, whose simulated spectra are shown in Figure 2, on the basis of comparisons with the published ^{1}H NMR spectra of the syn and anti conformers of [2.2]- and [3.3](1,4)-naphthalenophanes, and 1,8-di-(1-naphthyl)naphthalene.[13,15,16,20] The upfield shifts of *E,Ea* and *E,Es* versus **3** are consistent with the shielding expected for the face-to-face naphthyl rings, **3** being free of such interaction (see Figure 3). The 238 K spectrum of **1** can be simulated with a 1.0/0.6 ratio of *E,Es*/*E,Ea*, corresponding to a value of $\Delta G^\circ = 0.24$ kcal/mol at 298 K. Above and below 238 K, exchange broadening, chemical shift changes, and peak overlap prevent accurate spectral simulation of the aromatic region.[19] However, it is possible to calculate the activation barrier for interconversion of *E,Ea* and *E,Es* via Eyring treatment of exchange data obtained by iterative full line shape simulation of the aliphatic (*N*-methyl) region of the ^{1}H NMR spectra obtained between 248 and 268 K (Figure 4).[21] This analysis yields values of $\Delta G^\ddagger = 14$ kcal/mol ($\Delta H^\ddagger = 11.4 \pm$ kcal/mol and $\Delta S^\ddagger = 7.3 \pm 0.5$ cal/(mol deg)) for isomerization in either direction, in accord with the small difference in energy between the two conformers. A similar value of $\Delta G^\ddagger =$ 13 kcal/mol is obtained from the apparent coalescence temperature (263 K) and difference in frequency between the nonexchanging *N*-methyl chemical shifts (<248 K).

The value of $\Delta H^\ddagger$ for **1** is substantially larger than values reported for nitrogen−carbonyl single bond rotation (dihedral angle = ϕ) in urea (ca. 11 kcal/mol) and *N,N*′-dimethyl- and tetramethylurea (ca. 6 kcal/mol).[21] Further, this urea rotational process would not result in interconversion of *E,Ea* and *E,Es*.

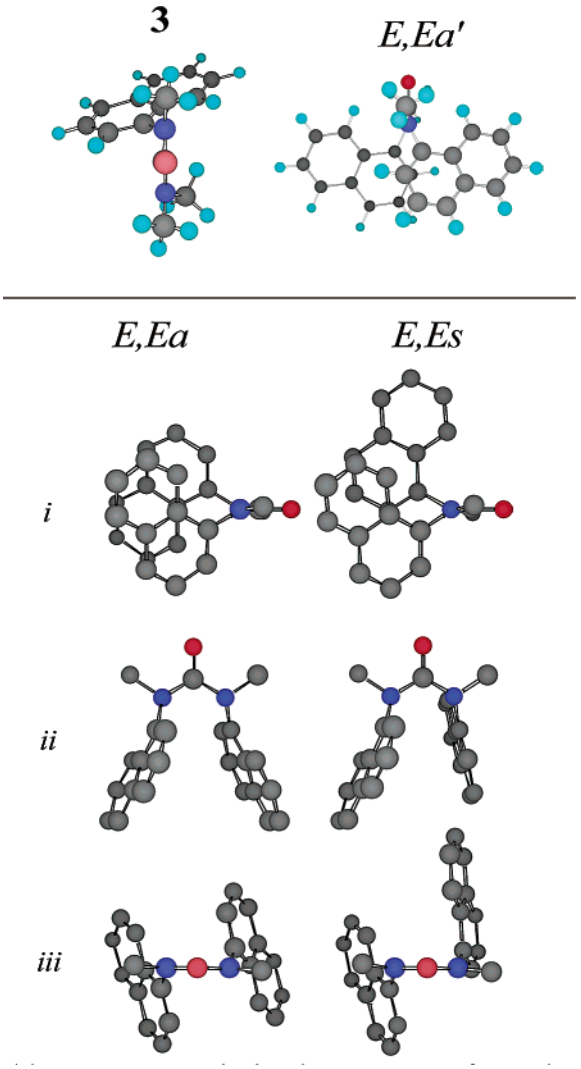

Figure 3. HF/6-31G** geometry optimized structures of **3** and *E,Ea*′ (top, left and right) and (bottom) syn (*E,Es*) and anti (*E,Ea*) conformations (shown without hydrogens); *i*, urea plane perpendicular to page; *ii*, urea plane in plane of page; *iii*, rotated 90° on the *x*-axis.

To our knowledge, the rotational barrier for a tertiary diarylurea has not been previously reported.

Theoretical Calculations. The energetics of syn−anti interconversion on *E,E*, *E,Z*, and *Z,Z* surfaces were initially explored via multidimensional PM5 calculations in which ϕ and the dihedral angle about a nitrogen−naphthalene bond, θ, are constrained to simulate rotation.[22] Structures and energies of the local minima were then fully optimized at the HF/6-31G** level.[23] Calculated structures for *E,Ea* and *E,Es* are shown from three perspectives in Figure 3. View *i* is parallel to the urea plane and reveals the large dihedral angles (C_4−N−N′−C_4′, ca. 63°) between the naphthyl short axes for both conformers. View *ii* is perpendicular to the urea plane and reveals the moderate splay angles (ca. 18°) between the short axes for each conformer. View *iii* is along the C═O bond and reveals the approximately parallel arrangement of the naphthalene long axes. The minimized geometry of *E,Ea* is similar to that of the crystal structure. The most pronounced difference is the larger

(20) (a) Wasserman, H. H.; Keehn, P. M. *J. Am. Chem. Soc.* **1969**, *91*, 2374. (b) Otsubo, T.; Boekelheide, V. *J. Org. Chem.* **1977**, *42*, 1085−1087.
(21) Haushalter, K. A.; Lau, J.; Roberts, J. D. *J. Am. Chem. Soc.* **1996**, *118*, 8891−8896.
(22) CAChe, 5.0, Fujistu Limited, Mihama-Ku, Chiba City, Chiba, Japan, 2000−2001.
(23) Jaguar, 4.0, Schrödinger, Inc., Portland, OR, 1991−2000.

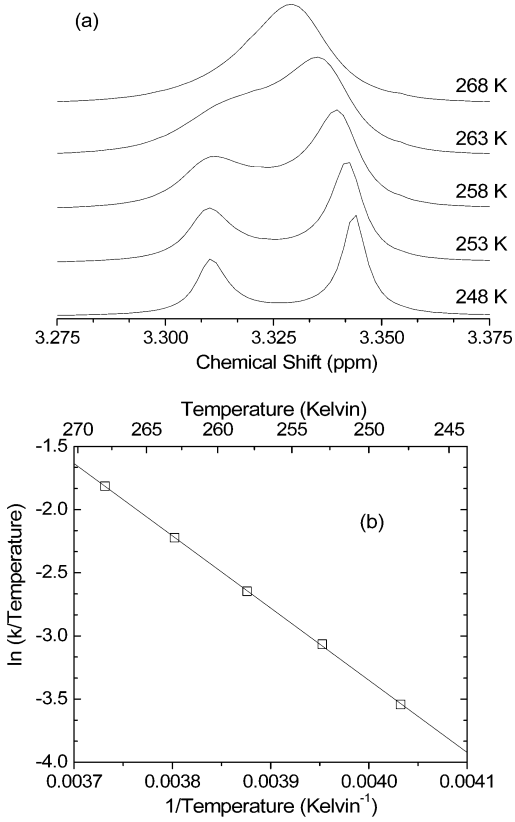

Figure 4. Temperature-dependent ^{1}H NMR spectra of the *N*-methyl signals of **1** (a). Corresponding exchange rate constant data and Eyring fit (b).

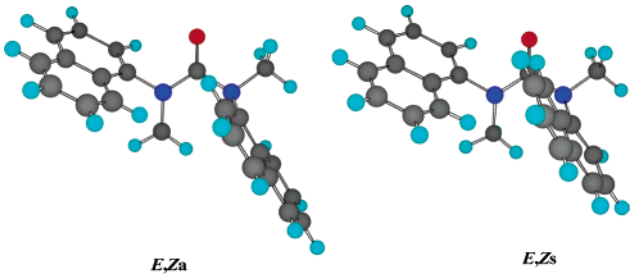

Figure 5. Optimized structures for *E*,*Zs* and *E*,*Za*.

splay angle for the calculated versus crystal structure (18° vs 12°), presumably due to the effect of crystal packing forces. The splay angles are similar to those for the more rigid 1,8-bis-(1-naphthyl)naphthalenes (18°).[15]

The calculated energy of *E*,*Es*, the global minimum, is lower than that of *E*,*Ea* by 0.6 kcal/mol, in accord with the relative energies determined by ^{1}H NMR. A slightly higher energy local minimum for *E*,*Ea* with less extensive π-overlap was also identified (Figure 3, *E*,*Ea*′). Local minima were also identified for two *E*,*Z* conformers of **1**, designated as *E*,*Zs* and *E*,*Za* (Figure 5). Their calculated energies are, respectively, 2.8 and 3.6 kcal/mol higher than that of *E*,*Es*, in agreement with the observation of only two sets of ^{1}H NMR signals for **1** at 238 K. The calculated energies of the *Z*,*Z* conformers of **1** are higher than those of the *E*,*Z* isomers. A local minimum was identified for the secondary urea **2**, having a *Z*,*Z* conformation similar to that of the crystal structure. The minimized structure for **3** shown in Figure 3 resembles that expected upon replacing one of the naphthyl groups of either *E*,*Ea* or *E*,*Es* by a methyl group.

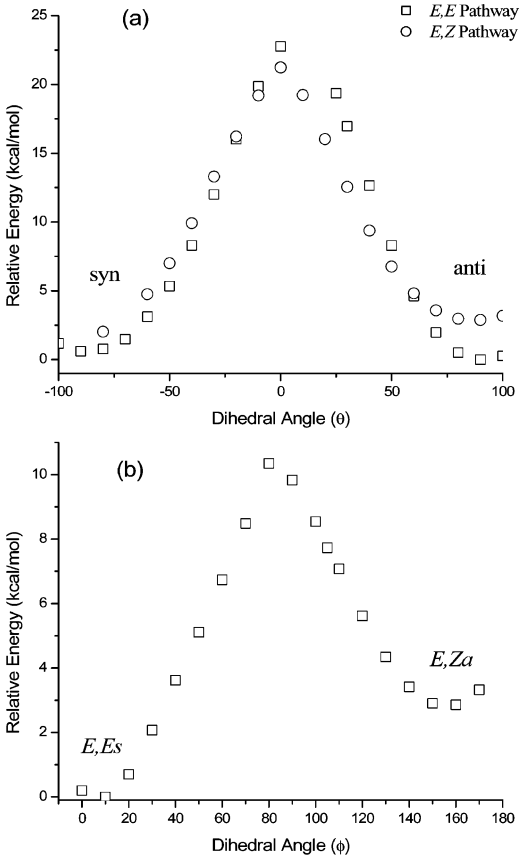

Figure 6. HF/6-31G** energy data depicting (a) the *E*,*E* and *E*,*Z* pathways to interconversion via rotation about the *N*-naphthyl bond θ. (b) Rotation about the *N*-carbonyl bond θ.

To determine the nature of the *E*,*Ea* and *E*,*Es* interconversion process, multiple series of singly constrained HF/6-31G** calculations were carried out. Starting from both *E*,*E* and *E*,*Z* geometries, θ was incrementally constrained to simulate rotation, while the remaining structure was fully optimized. The resulting energies are plotted in Figure 6a. Near the model transition state geometry, $\theta \approx 0$, the optimizations either converged to the corresponding "urea-flipped" (*E*,*E* to *E*,*Z* or *E*,*Z* to *E*,*E*) geometry or failed to converge. From these data, barriers of ca. 19 and 24 kcal/mol may be estimated for rotation about θ in both the *E*,*Z* and the *E*,*E* isomers, respectively (barriers correspond to rotation in the direction that results in *N*-Me/peri-hydrogen interaction). These barriers are similar to the experimental values for interconversion of the syn and anti isomers of 1,8-di-(1-naphthyl)naphthalene ($\Delta G^{\ddagger} = 27$ kcal/mol).[15] The slightly lower values for **1** are an indication of the ability of the urea linker to alleviate aryl−aryl interaction on the *E*,*Z* path and, to a lesser extent, on the *E*,*E* pathway. The calculated barriers are, however, much larger than that measured via ^{1}H NMR.

To further examine the conformational mobility of the urea linker, constrained optimizations, simulating rotation about ϕ, were carried out. The resulting energies allow estimation of the barrier to interconversion of *E*,*E* and *E*,*Z* conformations (ca. 10 kcal/mol, Figure 6b). This barrier is slightly higher than those previously reported for rotation of the dimethylamino group in either tetramethylurea or *N*,*N*′-dimethylurea (6−7 kcal/mol), but lower than those for rotation of either *N*-methylurea or the secondary diarylurea 1,3-di-(2-pyridyl)urea (11−12 kcal/mol).

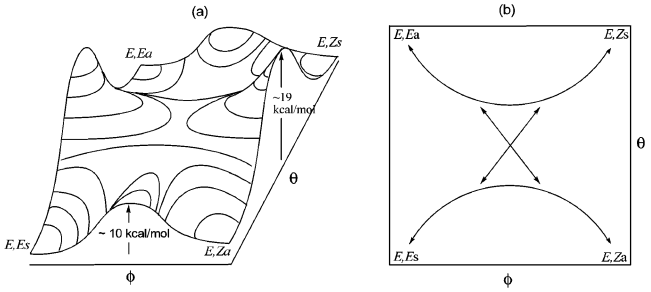

Figure 7. Depiction of the superposition of the potential energy surfaces of rotation about ϕ and θ, (a) contour diagram, (b) schematic top view.

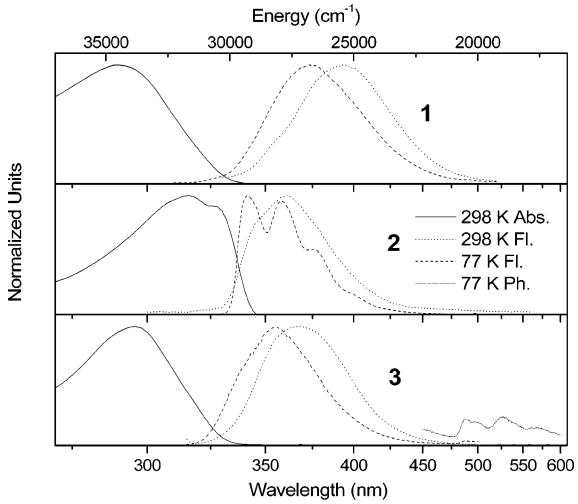

Figure 8. Absorption and emission spectra of **1**, **2**, and **3** at 298 and 77 K in m-THF.

Rotation about ϕ does not result in the interconversion of *E,Es* and *E,Ea* and thus cannot account for the experimental barrier.

The highest energy structures, $\phi \approx 0$ in Figure 6b, correspond to approximate model transition states for the *E,E* to *E,Z* conversion. In these geometries, the urea methyl group nearest the constrained rotation is approximately orthogonal to the carbonyl group of the linker. Structures near the model transition state for rotation about θ have similar urea geometries. The similarity of the model transition state geometries and the estimated barriers to rotation of ϕ or θ clearly suggests that the interconversion of *E,Es* and *E,Ea* is a concerted process. Hence, the lowest energy pathway for conversion of syn and anti conformers requires concurrent rotation about both ϕ and θ (Figure 7). We have not located a saddle point for such a process. However, its energy is expected to be somewhat higher than the barrier for rotation about ϕ, in accord with the value of $\Delta G^{\ddagger} = 14$ kcal/mol determined by NMR.

Electronic Spectra. The room-temperature UV absorption and emission spectra of ureas **1**−**3** both at room temperature and at 77 K in methyl-tetrahydrofuran (m-THF) are shown in Figure 8, and the spectral data are summarized in Table 2. The absorption maximum of **2** is at longer wavelength than those of **1** and **3**. This difference is attributed to conjugation between the coplanar naphthalene and urea orbitals of **2** (see Figure 1). The preferred folded geometries of **1** and **3** (Figures 3 and 4) and consequent loss in conjugation result in a blue-shift, loss of structure, and loss in intensity of the lowest energy $\pi-\pi^*$ transition. As previously suggested, the greater hypsochromism for urea systems such as **1** versus **3** may be a consequence of weak exciton coupling between the two naphthalene moieties.[7,16,24,25] The oblique angle between the two naphthalene transition dipoles should result in weak exciton coupling.[26]

Table 2. Absorption and Fluorescence Data of the 1-Naphthylureas[a]

urea	temp. (K)	λ_{abs}, nm	log ϵ	λ_f, nm	Φ_f	τ_s, ns
1	298	290	4.00	393	0.003	1.6
	77			373	0.50	11.5, 23
2	298	316	4.48	360	0.50	2.4
	77			340	0.89	2.4
3	298	296		367	0.10	1.1
	77			355	0.44	4.5

[a] Data acquired in deaerated m-THF solutions. Dual exponential fluorescence decay, preexponentials are 0.09 and 0.02, respectively. Phosphorescence also detected, $\lambda_p = 526$ nm, $\tau_p = 1.2$ s.

The fluorescence spectrum of **2** at 77 K has distinct vibronic structure, similar to that of naphthalene. Upon warming **2** to room temperature, the spectrum is broadened and the maximum is red-shifted to the position of the second vibronic band in the 77 K spectrum (Figure 8). The fluorescence quantum yield for **2** is large at both 77 and 298 K, and the fluorescence decay times at both temperatures are similar. The fluorescence of **3** is structureless at both 77 and 298 K and is red-shifted with respect to the fluorescence of **2**. Its fluorescence quantum yields and decay times are similar to those of **2**. Both **2** and **3** display weak phosphorescence at 77 K, with 0,0-bands at 500 nm and decay times of 1.5 and 1.2 ns, respectively.

The fluorescence of **1** is structureless and significantly red-shifted with respect to the spectra of either **2** or **3**. The red-shifted emission of **1** is attributed to an intramolecular excimer formed upon excitation of either *E,Ea* or *E,Es*. The absence of monomer fluorescence at 77 K indicates that **1** exists exclusively in folded conformations. The excitation and emission spectra of **1** are independent of the emission or excitation wavelength, respectively, at both 298 and 77 K. This is as expected, because the emission spectra of intramolecular excimers are known to be relatively insensitive to excimer geometry.[27] The 298 K fluorescence quantum yield for **1** is substantially smaller than those of **2** or **3**, suggestive of an efficient nonradiative decay channel for the singlet excimer. Neither monomer nor excimer phosphorescence emission is detected from **1** at 77 K ($\Phi < 10^{-3}$).

The fluorescence decay of **1** is best fit as a monoexponential function at 298 K but as a dual-exponential function below 200 K. The temperature dependence of the two component lifetimes is shown in Figure 9. The short-lived component has the larger preexponential and thus can be assigned to the major conformer, *E,Es*, if it is assumed that both components have similar radiative rates. Further assuming that there is only one activated singlet state decay process for each conformer, activation parameters can be obtained for that process by nonlinear fitting of the

(24) Todesco, R.; Gelan, J.; Martens, H.; Put, J.; De Schryver, F. C. *Tetrahedron* **1983**, *39*, 1407−1413.
(25) Yoshinaga, M.; Otsubo, T.; Sakata, Y.; Misumi, S. *Bull. Chem. Soc. Jpn.* **1979**, *52*, 3759−3760.
(26) Cantor, C. R.; Schimmel, P. R. *Techniques for the study of biological structure and function*; W. H. Freeman: San Francisco, 1980.
(27) Tsuchida, A.; Ikawa, T.; Tomie, T.; Yamamoto, M. *J. Phys. Chem.* **1995**, *99*, 8196−8199.

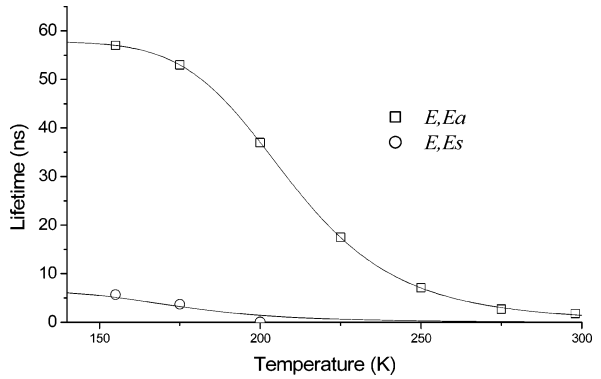

Figure 9. Temperature-dependent fluorescence decay times and Arrhenius fits for *E,Es* and *E,Ea* in m-THF.

Scheme 1

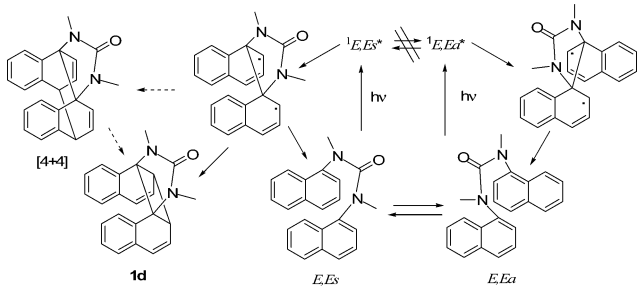

lifetime data (Figure 9) using eq 1,

$$\tau(T) = 1/[\sum k + A \exp(E_a/RT)] \qquad (1)$$

where $\sum k$ is the sum of all nonactivated processes (fluorescence and intersystem crossing), and A and E_a are the preexponential and activation energy of the activated process. The resulting values for *E,Es* are $\log A = 3.4 \times 10^{10}$ and $E_a = 3.5$ kcal/mol and for *E,Ea*, $\log A = 3.4 \times 10^{10}$ and $E_a = 5.1$ kcal/mol.

With **3** as a model for the monomer fluorescence of a tertiary 1-naphthylurea, the calculated monomer−excimer frequency shift for *E,Ea* at 298 K is $\Delta\nu = 1800$ cm^{-1}. This value is rather modest when compared to values of ca. $\Delta\nu = 5800$ cm^{-1} for both 1,3-di-(1-naphthyl)propane and di-(1-naphthylmethyl)-ether.[10,17] The smaller value of $\Delta\nu$ for *E,Ea* undoubtedly reflects its inability to form a parallel sandwich structure without distorting the urea linker. Naphthalenophanes with anti conformations or splayed ground-state structures also display much smaller values of $\Delta\nu$ than do structures with parallel syn naphthalene rings.[28] A larger value of $\Delta\nu$ might be expected for *E,Es* versus *E,Ea*; however, *E,Es* is nonfluorescent at room temperature.

Photochemical Reactions. Irradiation of **1** at room temperature in cyclohexane solution, as monitored by GC/MS or HPLC/UV chromatography, results in isolation of only the intramolecular [2+2] dimer (**1d**, Scheme 1), which is, of necessity, formed from *E,Es*. Analysis of irradiated solutions by ^{1}H NMR (Figure 10) confirms that **1d** accounts for the consumption of **1**. The starting material is exchange broadened, while no conformational mobility is detected for **1d**. After the sample was heated at 318 K for 1 h, the photodimer spectrum showed no change, indicating its stability toward thermal

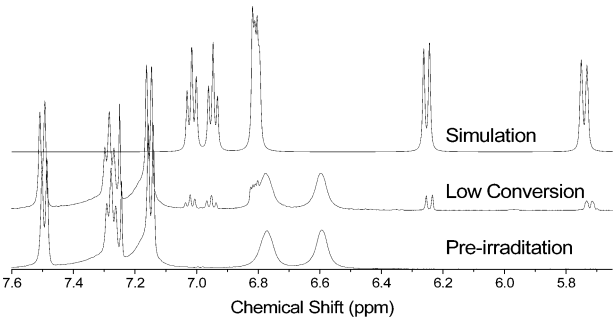

Figure 10. Dimerization of **1** in $CDCl_3$ at 298 K monitored by ^{1}H NMR, 500 MHz.

rearrangement. The quantum yield for formation of **1d** is 0.08. Because the room-temperature fluorescence quantum yield for **1** is 0.003 and no phosphorescence is observed at 77 K, we conclude that the singlet state decays of *E,Es* and *E,Ea* must be dominated by activated nonradiative processes.

The photochemical behavior of **1** is analogous in some respects to that of the corresponding diarylalkanes and cyclophanes. Irradiation of bis-(1-naphthylmethyl)ether yields both anti and syn [4+4] adducts with a total quantum yield of 0.04.[17] The syn, but not the anti, [4+4] adducts can undergo a thermal Cope rearrangement to yield the [2+2] or Cope dimers.[17,24] Only the Cope dimer is isolated upon intermolecular dimerization of 1-substituted naphthalenes at −78 °C.[29] The [4+4] dimerization of [2.2](1,4)(9,10)anthracenophane has a barrier of 3.3 kcal/mol, similar to the barrier for activated nonradiative decay of *E,Es*.[11]

A mechanism which accounts both for dimer formation from *E,Es*, but not *E,Ea*, and for the low quantum yield for dimer formation is outlined in Scheme 1. Nonsynchronous bonding at the naphthalene C_1 positions yields singlet diradical intermediates, which can partition between [2+2] and [4+4] adducts or return to starting dinaphthylurea. In the case of *E,Es*, the [4+4] adduct has a calculated energy 18 kcal/mol (HF/6-31G**)[23] higher than that of the [2+2] adduct, in accord with the formation of **1d** but not the [4+4] adduct. The singlet diradical of *E,Ea* is unable to form a [2+2] adduct and presumably decays predominantly by return to the dinaphthylurea. Alternatively, both *E,Es* and *E,Ea* may form highly strained [4+4] adducts that are thermally unstable and undergo Cope rearrangement (in the case of *E,Es*) or revert to the dinaphthylurea.[25] The large naphthalene−naphthalene splay angle in the ground state of **1** favors a nonsynchronous mechanism. The lower value of E_a for *E,Es* versus *E,Ea* presumably reflects the lower barrier for biradical formation from *E,Es* and accounts for the absence of room-temperature fluorescence from *E,Es*.

Concluding Remarks

In summary, the preferred folded geometry of tertiary diarylureas and the moderately large barrier for the interconversion of *E,Es* and *E,Ea* allow the characterization of the spectroscopy and photochemistry of both conformations. Kinetic modeling of the temperature dependence of the fluorescence lifetimes provides barriers of 3.5 and 5.1 kcal/mol for the activated nonradiative decay of the excimers of *E,Es* and *E,Ea*,

(28) Yanagidate, M.; Takayama, K.; Takeuchi, M.; Nishimura, J.; Shizuka, H. *J. Phys. Chem.* **1993**, *97*, 8881−8888.

(29) Noh, T.; Jeong, Y.; Kim, D. *J. Chem. Soc., Perkin Trans. 1* **1998**, 2501−2504.

respectively. These barriers are attributed to the nonsynchronous bonding in the singlet excimer and the resulting biradical partitioning between [2+2] dimer formation and return to starting material.

The behavior of **1** differs in several respects from that of its 2-naphthyl isomer.[7] No line-broadening is observed in the room-temperature ^{1}H NMR spectrum of the 2-naphthyl isomer, indicative of a lower barrier for interconversion of syn and anti conformers. In addition, the 77 K fluorescence of the 2-naphthyl isomer shows little broadening or frequency shift as compared to that of naphthalene and thus is assigned to the locally excited monomer. This is also the case for the other tertiary diarylureas that we have examined.[6,7] The unique ability of **1** to form an excimer at 77 K in a rigid glass is attributed to its ground-state geometry, which is more appropriate for excimer formation than those of other tertiary diarylureas.

Tertiary diarylureas such as **1** can be used as building blocks for the formation of extended arrays of aromatic rings connected by urea linkers. The preferred π-stacked "protophane" geometries and conformational flexibility of the urea linker allow for optimized excited-state interactions between adjacent π-chromophores. The ease of construction of both homo−arene arrays and donor−bridge−acceptor arrays makes the tertiary ureas attractive candidates for the design of wirelike molecules that mimic the properties of the π-stacked base pairs in DNA.

Experimental Section

General Data. ^{1}H NMR spectra were recorded in $CDCl_3$ solutions using an Inova 500 spectrometer with TMS as an internal standard. The instrument was calibrated using a methanol sample, and temperatures are accurate to ±1 °C. Spectral simulations and exchange calculations were performed using gNMR version 4.1 for Windows.[30] Silica gel was used for analytical and gravity flash chromatography. Melting points are uncorrected.

Single crystals of **1** and **2** were obtained by slow evaporation of hexanes/ethyl acetate and DMSO, respectively. Data for the X-ray structure of **1** was recorded using a Bruker SMART-1000 CCD area detector with graphite monochromated Mo Kα radiation. Measurements of **2** were made on a MAR CCD area detector with graphite monochromated Mo Kα radiation at the Advanced Photon Source at DND-CAT. The structures were solved via direct methods and expanded using Fourier techniques. For **1a**, the non-hydrogen atoms were refined anisotropically, but those of **2** were refined isotropically. Data were collected and processed using SMART-NT and MAR, and SAINT-NT programs. Numerical details pertaining to the collection of data, data processing, and refinement of the structures are given in Table 1 and in the .cif files included in the Supporting Information.

UV−vis spectra were measured on a Hewlett-Packard 8452A diode array spectrometer using a 1 cm path length quartz cell. Total emission spectra were measured on a SPEX Fluoromax spectrometer. Low-temperature spectra were measured either in a Suprasil quartz EPR tube (i.d. = 3.3 mm) using a quartz liquid nitrogen coldfinger dewar at 77 K or in an Oxford Cryogenics DN1704 cryostat fitted with an Oxford Instruments ITC4 temperature controller. Total emission quantum yields were measured by comparing the integrated area under the total emission curve at an equal absorbance and the same excitation wavelength as an external standard, 9,10-diphenylanthracene ($\Phi_f \approx 1.0$ at 77 K in m-THF). All emission spectra are uncorrected, and the estimated error for the quantum yields is ±10%.

Fluorescence decays were measured on a Photon Technologies International (PTI) Timemaster stroboscopic detection instrument with a gated hydrogen or nitrogen lamp using a scatter solution to profile the instrument response function. Phosphorescence decays were measured on a PTI Timemaster phosphorescence time-based-detection instrument excited with a xenon-flash lamp as the excitation source. Nonlinear, least-squares fitting of the decay curves employed the Levenburg−Marquardt algorithm as described by James et al. and implemented by the Photon Technologies International Timemaster (version 1.2) software.[31] Goodness of fit was determined by judging the χ^2 (<1.3 in all cases), the residuals, and the Durbin−Watson parameter (>1.6 in all cases). Solutions were degassed under vacuum (<0.1 Torr) through five freeze−pump−thaw cycles.

PM5 optimizations were performed using CAChe version 5.0 for windows.[22] Constrained and unconstrained ab initio HF/6-31G** calculations were performed using Jaguar version 4.1 for Linux.[23]

Materials. Triphosgene, triethylamine, 1-aminonaphthalene, dimethylamine hydrochloride, and iodomethane are commercially available and were used as received. Hexanes, ethyl acetate, and DMSO were spectroscopic grade and were used as received from Aldrich.

***N,N′*-Di-1-naphthylurea, 2.** To a solution of 1-naphthylamine (10 mmol) in dichloromethane (20 mL) was added 2.2 equiv of triethylamine, followed by 1.6 mmol of triphosgene. After the mixture had been stirred for 10 min, the solvent was removed using a rotary evaporator. The solid residue was washed with water and recrystallized from DMF−water (10:1). The resulting crystalline amide was washed with water and dried under vacuum: mp 299 °C (with some decomposition above 290 °C). ^{1}H NMR (DMSO-d_6, 500 MHz): δ 9.169 (2H, s), 8.237 (2H, d), 8.072 (2H, d), 7.948 (2H, d), 7.649 (2H, d), 7.632 (2H, t), 7.564 (2H, t), 7.493 (2H, t) (all couplings simulated sufficiently by 8.0 Hz). MS: *m*/*z* 312.1 (M^+).

***N,N*-Dimethyl-*N,N′*-di-1-naphthylurea, 1.** Into a solution of *N,N′*-1-naphthylurea (10 mmol) in DMF (20 mL) was added dropwise 1.5 equiv of NaH in 10 mL of DMF, followed by 1.5 equiv of MeI. The mixture was stirred at room temperature until the starting material had been consumed (ca. 2−3 h), and was then mixed with water and extracted with CH_2Cl_2. The organic layer was washed with water and dried with anhydrous potassium carbonate. After the solvent had been removed, the residue was purified by column chromatography using mixed solvent (acetone and hexane) to afford **1**: mp 136−137 °C. ^{1}H NMR ($CDCl_3$, 25 °C, 500 MHz): δ 3.48 (6H, s), 6.83 (br. s), 6.99 (br. s), 7.36 (br. d), 7.51 (br. m), 7.70 (br. d). MS: *m*/*z* 340.1 (M^+).

***N,N,N′*-Trimethyl-*N′*-1-naphthylurea, 3.** To a solution of 1-aminonaphthalene (0.66 g, 3 mmol) in dichloromethane (20 mL) was added 1.4 mL of triethylamine (10 mmol), followed by 0.3 g of triphosgene (1 mmol). After the mixture had been stirred for 30 min, a mixture of 0.6 g of dimethylamine hydrochloride (7 mmol), 1.4 mL of triethylamine (10 mmol), and 20 mL of dichloromethane was added. The mixture was refluxed for 10 min, and the solvent was removed using a rotary evaporator. The solid residue was washed with water and recrystallized from acetone−hexane (1:1) to give 0.8 g (90%) of *N,N*-dimethyl-*N′*-1-naphthylurea: mp 170−171 °C. ^{1}H NMR ($CDCl_3$, 500 MHz): δ 3.11 (6H, s), 6.61 (1H, s), 7.47 (1H, t, J = 8.0, 7.0 Hz), 7.63 (1H, J = 6.0 Hz), 7.75 (1H, d, J = 7.0 Hz), 7.44 (1H, t, J = 7.0, 8.0 Hz), 7.49 (1H, t, J = 7.0, 8.0 Hz), 7.84 (1H, t, J = 1.0, 8.0 Hz), 7.84 (1H, t, J = 2.0, 8.0 Hz). MS: *m*/*z* 214.1 (M^+). This was methylated with MeI−NaH as described above to afford **3**, which was purified by column chromatography to give colorless crystals in 60% yield: mp 122−123 °C. ^{1}H NMR ($CDCl_3$, 500 MHz): δ 3.20 (3H, s), 2.55 (3H, s), 7.40 (1H, t, J = 8.0, 8.0 Hz), 7.18 (1H, t, J = 1.5, 8.0 Hz), 7.72 (1H, t, J = 1.5, 8.0 Hz), 7.51 (1H, m, J = 1.5, 8.0, 8.0 Hz), 7.55 (1H, m, J = 1.5, 8.0, 8.0 Hz), 7.87 (1H, t, J = 1.5, 8.0 Hz), 8.01 (1H, t, J = 1.5, 8.0 Hz). MS: *m*/*z* 228.1 (M^+).

Intramolecular Photodimerization. Deaerated cyclohexane solutions were irradiated in a Rayonet Photoreactor fitted with 300 nm lamps

(30) gNMR, 4.1, Adept Scientific plc, Herts, U.K., 1995−1999.

(31) James, D. R.; Siemiarczuk, A.; Ware, W. R. *Rev. Sci. Instrum.* **1992**, *63*, 1710−1716.

or with a PTI Optical Bench with 290 nm light from a Hg−Xe arc lamp. Stilbene was used as an external standard for the measurement of the quantum yield of product formation. Monitored via UV/vis spectroscopy, samples of both stilbene and **1** had an O.D. of 0.11 at 290 nm. Product formation was also monitored in concentrated samples via GC/MS and ^{1}H NMR. At low and high conversion, one major product **1d** was formed. ^{1}H NMR ($CDCl_3$, 500 MHz): δ 2.69 (3H, s), 3.77 (1H, s), 5.72 (1H, m, J = 9.5, 1.8, 1.7 Hz), 6.24 (1H, d, J = 2.0 Hz), 6.8−7.0 (2H, m), 6.95 (1H, t, J = 8.0, 7.0 Hz). MS: m/z 341.4 $(M + H)^+$, 340 M^+.

Acknowledgment. We thank C. L. Stern for X-ray analysis of the crystal structures. Funding for this project was provided by NSF grant CHE-0100596.

Supporting Information Available: Variable-temperature ^{1}H NMR spectra (aryl region) of **1** (PDF) and .cif files for **1** and **2**. This material is available free of charge via the Internet at http://pubs.acs.org.

JA034311W